

Supplementary Information for

The contribution of host cell-directed vs. parasite-directed immunity to the disease & dynamics of malaria infections.

Nina Wale, Matthew J. Jones, Derek G. Sim, Andrew F. Read, Aaron A. King

Corresponding Author Nina Wale.
E-mail: nwale@umich.edu

This PDF file includes:

- Supplementary text
- Figs. S1 to S4
- Table S1
- References for SI reference citations

Supporting Information Text

Experimental methods: further details

Assaying RBC demography using flow cytometry. We used flow cytometry to measure the proportion of reticulocytes (young RBCs) and erythrocytes (mature RBCs) in the blood. Reticulocytes express the CD71 receptor, which is lost upon their maturation into erythrocytes (1, 2); all cells in the erythroid lineage express the TER119 antigen (3). Thus, staining with distinctly-tagged TER-119 and CD71 antibodies can be used to isolate the RBC portion of the blood and measure the relative abundance of reticulocytes and erythrocytes (4).

Blood was stained with TER-119 and CD71 antibodies labelled with distinct fluorophores. Briefly, 2 μl blood was collected in 48 μl running buffer (phosphate buffer saline with 2 mM Ethylenediaminetetraacetic acid and 2% fetal bovine serum). Cells were mixed with 50 μl of each of three different solutions: FITC anti-mouse CD71 (Biolegend 113805), PE anti-mouse TER-119 (Biolegend 116207), APC anti-mouse CD41 (Biolegend 133914), for final concentrations of 0.005, 0.0025, and 0.0025 $\mu\text{g}/\mu\text{l}$, respectively. Samples were vortexed and incubated for an hour at 4C in the dark, washed with 1 ml of running buffer and centrifuged at 2000 rpm for 5 min. The supernatant was then decanted and the pellet resuspended to a final concentration of 10^7 cells/ μl .

Stained samples were analyzed using a FlowSight Imaging Flow Cytometer (Amnis) with specifications described in Table S-1. 300,000 events were counted per sample and analysis performed using IDEAS software (Amnis, version 6), as follows. RBCs were distinguished from platelets and cell debris by their size (area) and CD41⁺ status. Single cells were then distinguished from doublets on the basis of their major axis (the longest dimension of the cell) and density (side-scatter). The population of single, TER119⁺ cells was then plotted in TER119/CD71 space and reticulocytes (CD71⁺) cells gated from erythrocytes (CD71⁻) using a gate drawn using fluorescence minus one (FMO) controls (RBCs stained with the CD41 and TER119 antibodies but not CD71). Single color (1000 events), FMO and unstained (5000 events) controls were generated from the blood of uninfected mice and run prior to sample analysis, daily. On days 11–14 samples were not stained with the CD41 antibody, as this reagent was unavailable.

We multiplied daily measures of the proportion of reticulocytes and erythrocytes, as derived as above, by the total RBC density to obtain the density of reticulocytes and erythrocytes on each day (Fig. S-1).

Mathematical modeling: further details

Calculating the contribution of the different host response components to parasite fitness and host disease. We begin by making the definitions

$$S_t^M = \exp\left(-\frac{M_t}{R_t + E_t}\right), \quad S_t^N = \exp\left(-\frac{N_t}{R_t + E_t}\right), \\ S_t^W = \exp\left(-\frac{W_t}{R_t + E_t}\right).$$

Now, to quantify the relative contribution of the indiscriminate killing response, targeted response, and parasites to RBC destruction (as shown in Figs. 3C & S-3), we calculate the following quantities that collectively sum to 1:

$$Q_t^{ps} = (1 - S_t^M) S_t^W S_t^N, \\ Q_t^{pn} = \frac{N_t}{N_t + W_t} (1 - S_t^M) (1 - S_t^W S_t^N), \\ Q_t^{pw} = \frac{W_t}{N_t + W_t} (1 - S_t^M) (1 - S_t^W S_t^N), \\ Q_t^{un} = S_t^M (1 - S_t^N), \\ Q_t^{us} = S_t^M S_t^N.$$

Here, Q_t^{ps} is the fraction of RBCs infected and destroyed by parasites emerging from them, Q_t^{pn} the fraction parasitized and destroyed by indiscriminate killing, Q_t^{pw} the fraction parasitized and destroyed by targeted killing, Q_t^{un} the fraction that go uninfected but are nevertheless destroyed by indiscriminate killing, and Q_t^{us} is the fraction of RBCs that survive in the preceding 24 hr.

To quantify parasite fitness, as in Figs. 3A & S-3, we divide the per-merozoite reproductive potential into five components:

$$\lambda_t^r = \beta \frac{R_t}{M_t} Q_t^{ps}, \quad \lambda_t^e = \beta \frac{E_t}{M_t} Q_t^{ps}, \\ \lambda_t^n = \beta \frac{R_t + E_t}{M_t} Q_t^{pn}, \quad \lambda_t^w = \beta \frac{R_t + E_t}{M_t} Q_t^{pw}, \\ \lambda_t^u = \beta - \lambda_t^r - \lambda_t^e - \lambda_t^n - \lambda_t^w.$$

Here, λ_t^r and λ_t^e are the numbers of offspring that find and successfully reproduce within reticulocytes (immature RBCs) and erythrocytes (mature RBCs), respectively. On the other hand, we have λ_t^n , which is the unrealized potential due to destruction of parasitized cells by the indiscriminate response; λ_t^w , that due to destruction of parasitized cells by the targeted response; and λ_t^u , that due to lack of RBC availability. Note that $(\lambda_t^r + \lambda_t^e) M_t = M_{t+1}$ and $\lambda_t^r + \lambda_t^e + \lambda_t^n + \lambda_t^w + \lambda_t^u = \beta$.

A. Calculating net change in RBC density. In general, anemia is the result of both (i) the destruction of RBCs and (ii) deficiency in their supply; if the two are balanced, then RBC concentrations remain unchanged. In Figs. 3B & S-3, we compared the previous day’s RBC losses, with reticulocyte supply on the following day, computing

$$R_t - (R_{t-1} + E_{t-1}) (1 - Q_{t-1}^{us}).$$

We interpret this quantity as a surplus or deficit according to whether it is positive or negative.

B. Model fitting and smoothing. We began by estimating the ten parameters independently for each mouse using 150 IF2 iterations of 10000 particles. Then, excluding the uninfected mice, we ran 400 iterations of the panel IF2 algorithm (5) using 20000 particles, from each of 250 starting points distributed inside a large box in the 10-dimensional search space. We observed that these algorithms gave estimates clustered in a narrow region of parameter space relative to that spanned by the starting points. To further refine the estimates, we computed a likelihood profile over σ_W , maximizing the likelihood over the remaining parameters at each of 100 values of that parameter. This was accomplished by starting 10 independent IF2 algorithms at each of 100 gridded σ_W values. Each independent IF2 consisted of 3 rounds of 100 iterations of 10000, 20000, and 40000 particles, respectively. The highest observed likelihood overall was taken to be the maximum likelihood estimate (MLE). Smoothed estimates of the state variables were obtained by running 2000 independent particle filter calculations, each using 10^5 particles, and extracting a single trajectory from each one.

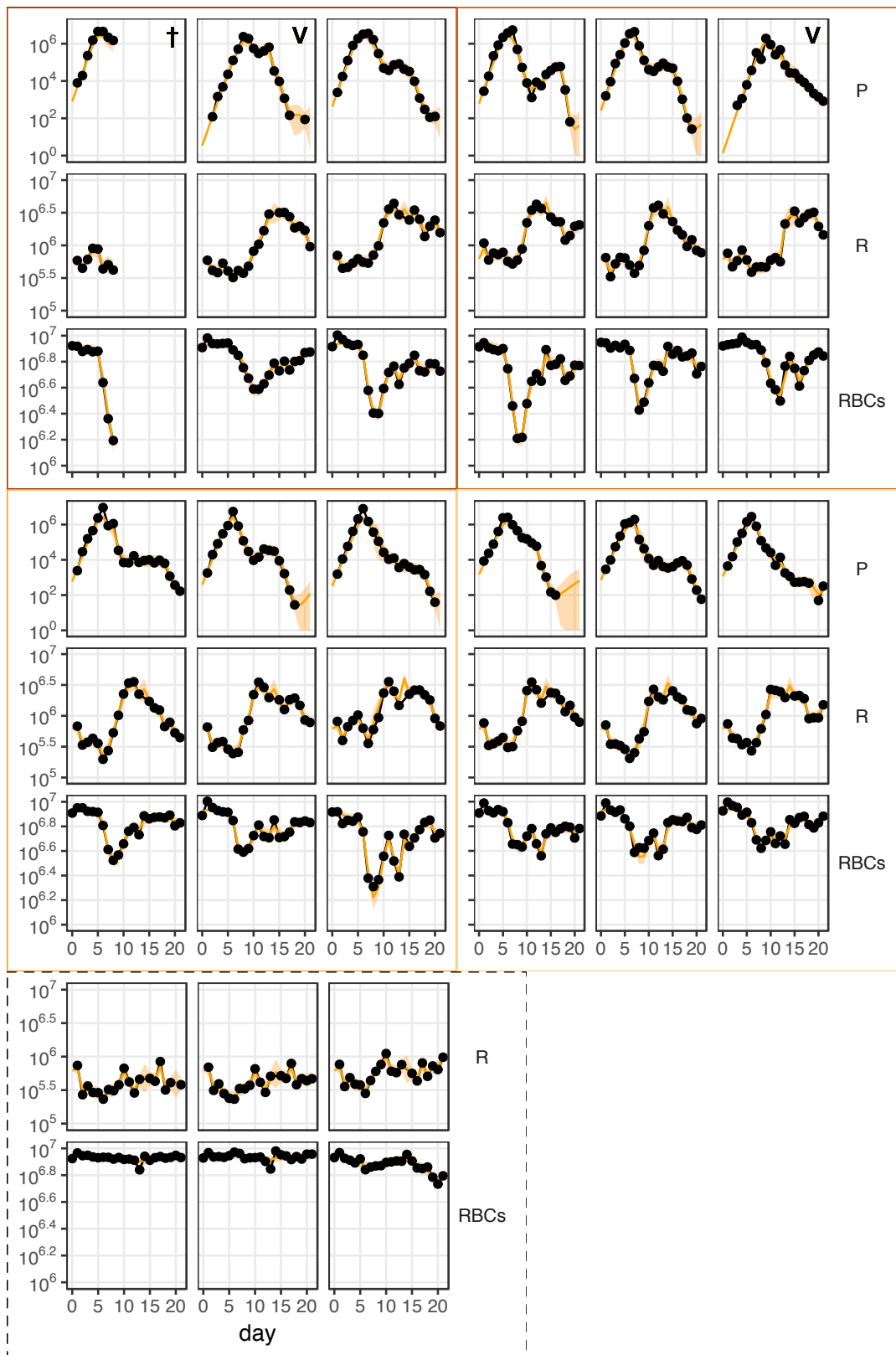


Fig. S-1. Data and fitted model trajectories of each mouse in the study. The density of parasites (P), reticulocytes (R) and total RBCs (RBCs) through time in the fifteen mice used in this study. The model (orange, smooth line) captures the data (black) well, in all cases. Twelve mice (plots with solid border) were infected with one million *Plasmodium chabaudi* parasites. These twelve infected mice were split into four groups of three that received as drinking water a 0.05% (top left block, brown border), 0.005% (top right, light brown border), 0.0005% (middle left, orange border) or 0% (middle right, yellow border) solution of pABA, respectively. Three further mice were left uninfected (bottom left, dashed border). One mouse died (indicated by †) and two received fewer parasites than was intended (V).

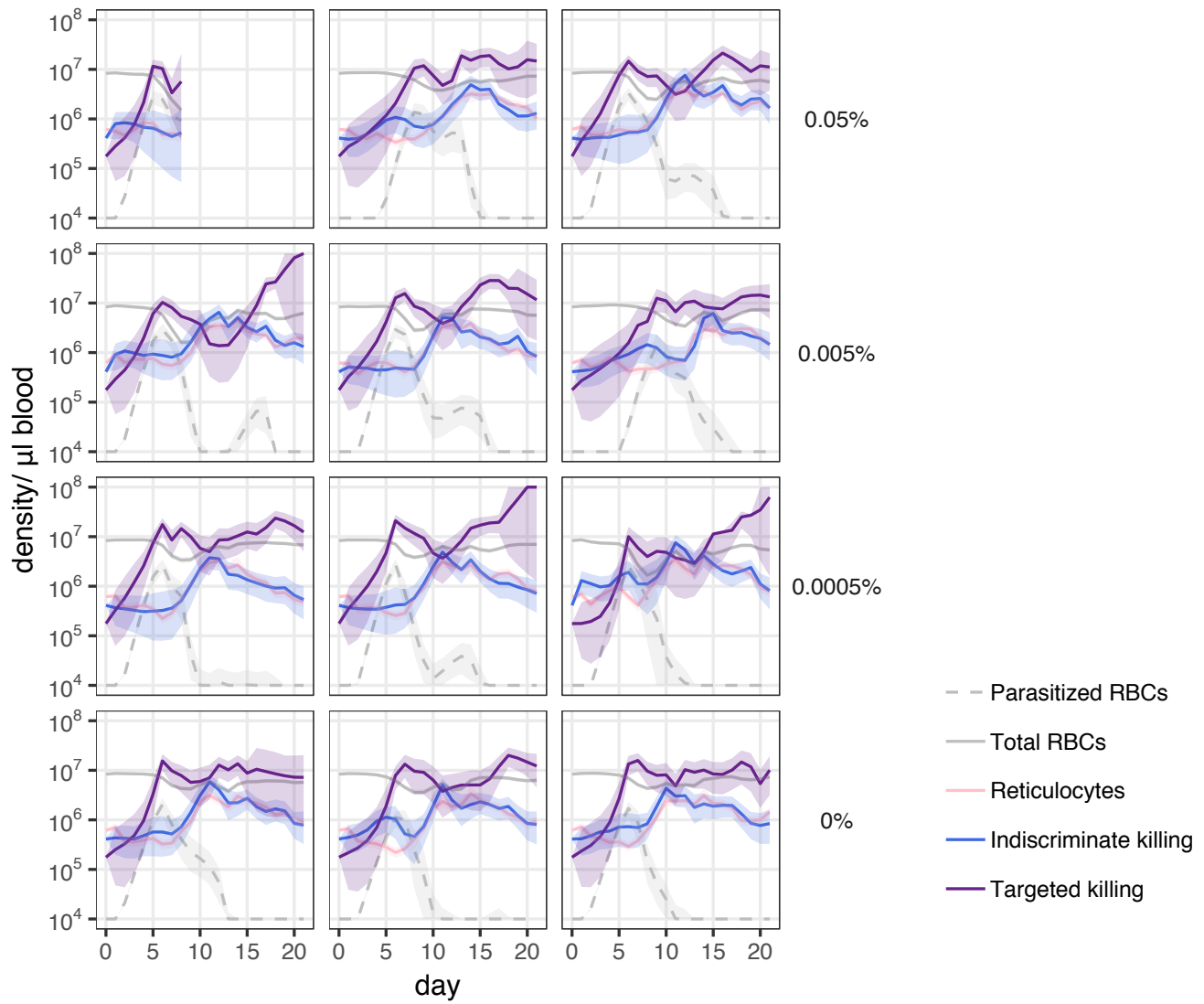


Fig. S-2. Fitted trajectories of the three components of the immune response. The trajectory of the targeted killing response (purple), indiscriminate killing response (blue) and supply response (pink) in each of 12 infected mice; the estimated densities of total RBCs (smooth line) and parasites (dashed line) are shown in grey. Plotted are the mean (solid line) and 90% confidence interval (ribbon) on the smoothed estimate of the model trajectories. Each panel shows the dynamics in a single mouse. The concentration of pABA that each mouse received as drinking water is indicated on the right.

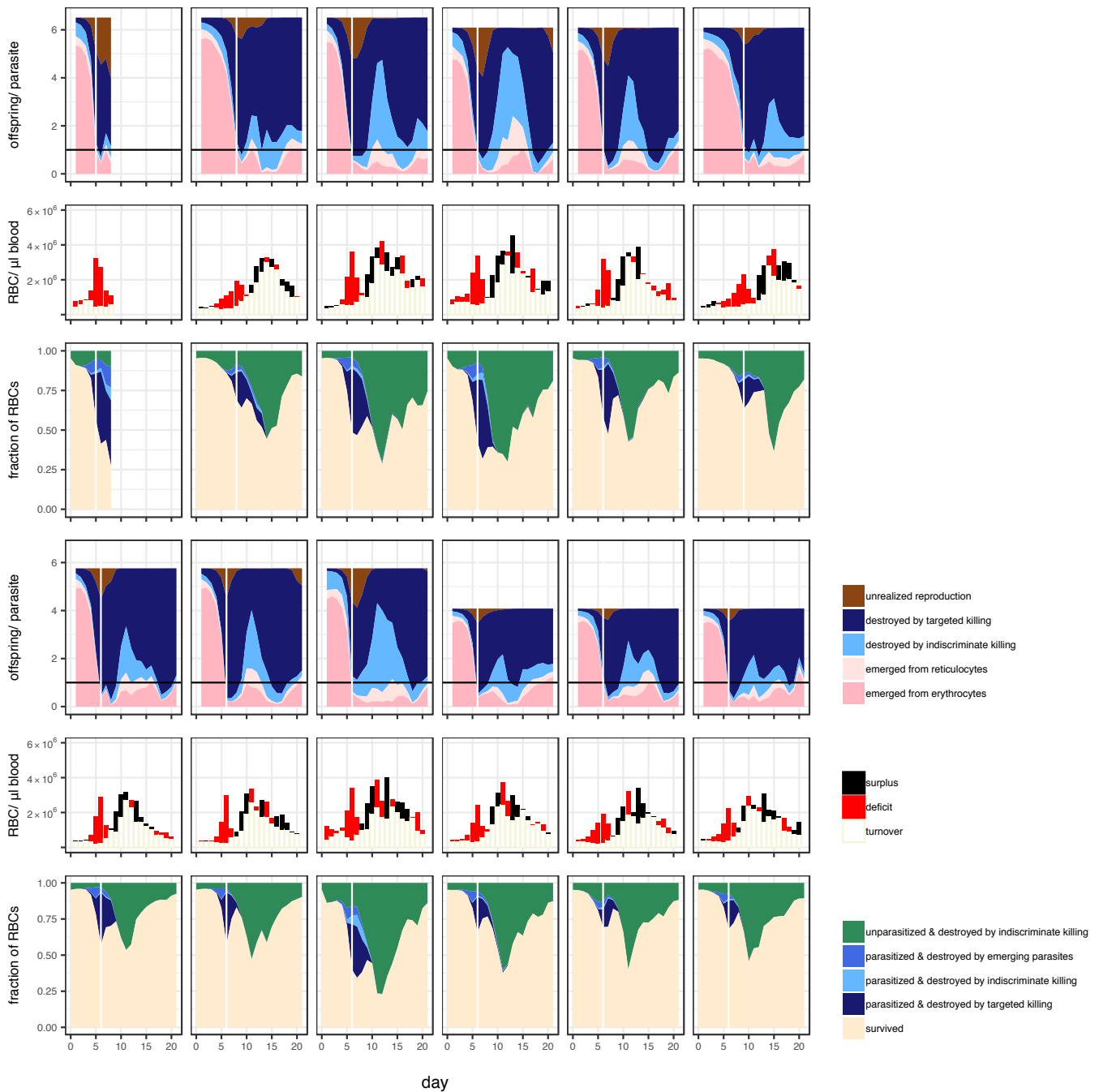


Fig. S-3. Contribution of the different components of the host response to parasite fitness and host disease in each infected mouse. Each column of three plots shows the analysis for a single mouse. First & Fourth row) Contribution of the host to (the suppression of) parasite reproduction. The height of the filled area indicates the maximum number of offspring that could be produced per parasitized cell in conditions of unlimited RBC availability. Fill color indicates the estimated number of offspring that successfully emerged (pinks), were destroyed by each of the killing responses (blues) or were not produced due to the limited availability of RBCs (brown). Black horizontal line indicates one offspring/parasite—when the blue area descends below this line the parasite population is decreasing in size. Second and Fifth Rows) Uncolored part of the bar indicates the number of the previous day's losses that were compensated for by the present day's supply of reticulocytes (turnover); The colored section indicates the extent to which the present day's supply of reticulocytes exceeded yesterday's losses ('surplus', black) or failed to compensate for them ('deficit', red). Third & Sixth Rows) The relative contribution of parasites and each of the host responses to the fate of RBCs through time. Note that parasites can contribute to RBC destruction directly, by emergence, or indirectly via the targeted killing response. White vertical line in A & C indicates the time of peak parasite density. Mice were administered a (top three rows, first three columns) 0.05%, (top three rows, last three columns) 0.005%, (bottom three rows, first three columns) 0.0005% and (bottom three rows, last three columns) 0% solution of pABA as drinking water.

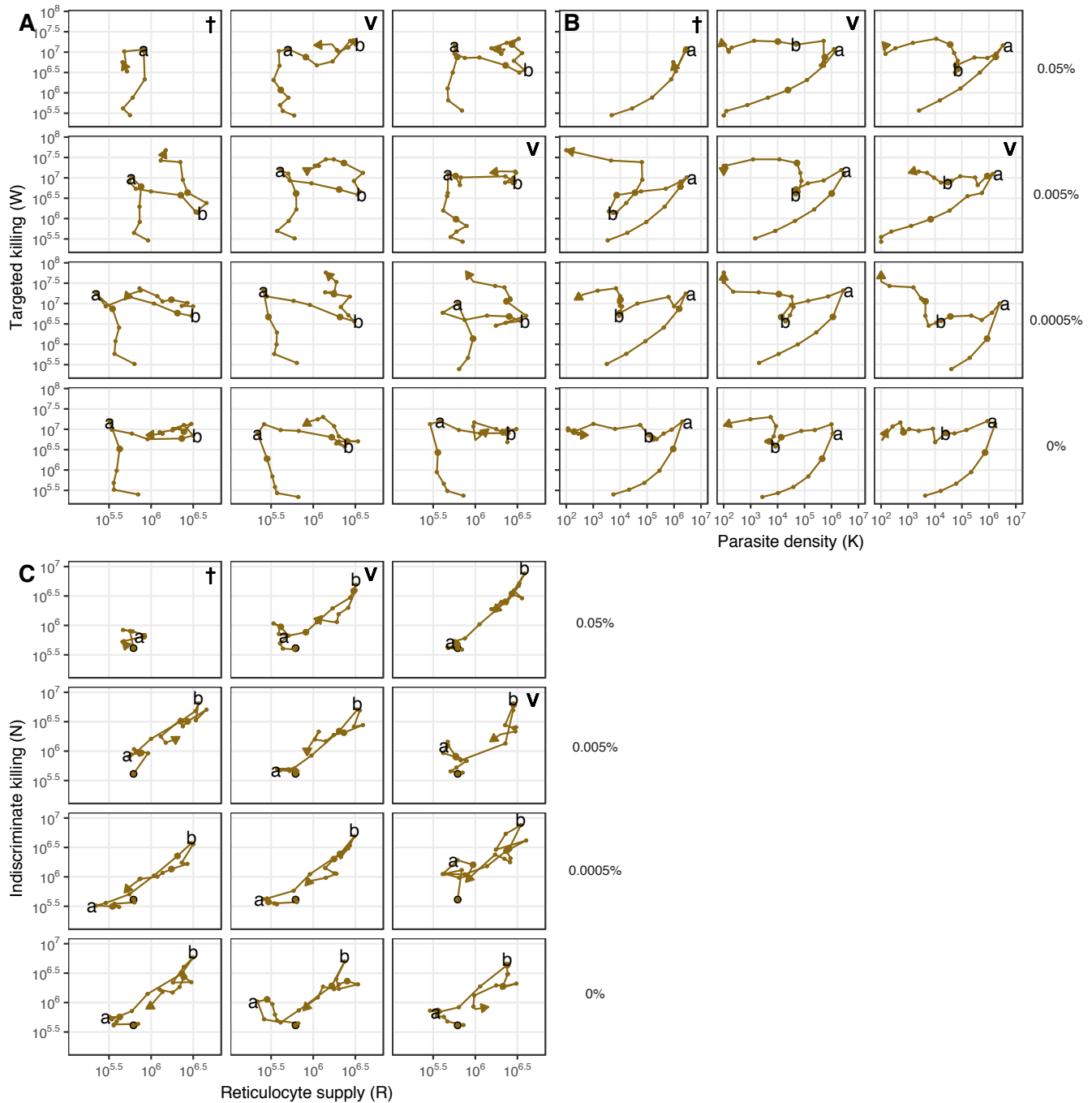


Fig. S-4. The components of the immune response are similarly deployed across mice. The relationships between A) reticulocyte density and targeted killing, B) parasite density and targeted killing and C) reticulocyte density and indiscriminate killing in infected mice given (top row) 0.05%, (second row down) 0.005%, (third row down) 0.0005% and 0% solution of pABA as drinking water. Landmarks **a** and **b** identify transitions between regimens of deployment of the components that occur. In each panel are shown the dynamics of a single mouse. The large, black-lined dot indicates the starting point of the infection; each subsequent day is marked with a dot, with large dots indicating days 5, 10, 15, 20. Densities of parasites and reticulocytes are in units per microliter of blood. Plotted are the median fitted trajectories, as estimated from the model. † indicates that the mouse died (and, as a result, its infection did not extend to landmark **b**), V that the mouse received fewer parasites than was intended.

Table S-1. Flow Cytometer setup

Channel	1	2	3	11
Laser, nm	NA	488	488	785
Emission Filters, nm	NA	430-480	505-560	560-595
Fluorochrome detected	NA	FITC	PE	APC

References

1. BT Pan, R Blostein, RM Johnstone, Loss of the transferrin receptor during the maturation of sheep reticulocytes in vitro. An immunological approach. *Biochem. J.* **210**, 37–47 (1983).
2. J Liu, X Guo, N Mohandas, JA Chasis, X An, Membrane remodeling during reticulocyte maturation. *Blood* **115**, 2021–2027 (2010).
3. T Kina, et al., The monoclonal antibody TER-119 recognizes a molecule associated with glycophorin A and specifically marks the late stages of murine erythroid lineage. *Br. J. Haematol.* **109**, 280–287 (2000).
4. M Koulis, et al., Identification and analysis of mouse erythroid progenitors using the CD71/TER119 flow-cytometric assay. *J. Vis. Exp.* **54**, e2809 (2011).
5. C Bretó, EL Ionides, AA King, Panel data analysis via mechanistic models. *J. Am. Stat. Assoc.* **in press** (2019).